

Data report: revised Pleistocene age model based on a modified nannofossil bioevent and additional measurements of benthic foraminiferal oxygen and stable carbon isotope ratios from Hole U1352B, offshore Canterbury Basin, New Zealand¹

Koichi Hoyanagi,² Yuichiro Tanaka,³ Tokinori Takeuchi,² Minoru Ikehara,⁴ Masayuki Utsunomiya,³
Peter Blum,⁵ Cecilia M. McHugh,⁶ and Craig S. Fulthorpe⁷

Chapter contents

Abstract	1
Introduction	1
Materials and methods	2
Results	3
Acknowledgments	4
References	4
Figures	6
Tables	12

¹Hoyanagi, K., Tanaka, Y., Takeuchi, T., Ikehara, M., Utsunomiya, M., Blum, P., McHugh, C.M., and Fulthorpe, C.S., 2018. Data report: revised Pleistocene age model based on a modified nannofossil bioevent and additional measurements of benthic foraminiferal oxygen and stable carbon isotope ratios from Hole U1352B, offshore

Canterbury Basin, New Zealand. In Fulthorpe, C.S., Hoyanagi, K., Blum, P., and the Expedition 317 Scientists, *Proceedings of the Integrated Ocean Drilling Program, 317: Tokyo* (Integrated Ocean Drilling Program Management International, Inc.). doi:10.2204/iodp.proc.317.210.2018

²Department of Geology, Institute of Science, Shinshu University, 3-1-1 Asahi, Matsumoto 390-8621, Japan. Correspondence author: hoya101@shinshu-u.ac.jp

³Geological Survey of Japan, AIST, 1-1-1 Higashi, Tsukuba 305-8567, Japan.

⁴Center for Advanced Marine Core Research, Kochi University, Nankoku 783-8502, Japan.

⁵International Ocean Discovery Program, Texas A&M University, College Station, TX 77845, USA.

⁶School of Earth and Environmental Sciences, Queens College, CUNY, 65-30 Kissena Boulevard, Flushing NY 11367, USA.

⁷University of Texas Institute for Geophysics, John A. and Katherine G. Jackson School of Geosciences, J.J. Pickle Research Campus, Building 196 (ROC), 10100 Burnet Road (R2200), Austin TX 78758-4445, USA.

Abstract

Reexamination of a nannofossil datum, the highest occurrence of *Pseudoemiliania lacunosa* (Zone NN20/NN19; 0.44 Ma), has led to a revised datum depth in Integrated Ocean Drilling Program Expedition 317 Hole U1352B. Furthermore, comparison between isotopic ratios of benthic foraminifers *Nanionella flemingi* and *Uvigerina perigrina* indicate that oxygen and carbon isotopic ratios for both species, when they occur in the same horizon, are almost identical. Therefore, we can correlate the oxygen isotopic variations of *N. flemingi* with the LR04 stack. We have conducted additional measurements of oxygen and stable carbon isotope ratios of *N. flemingi*, which in conjunction with our revised nannofossil datum allows a new correlation with the LR04 stack and results in revision of our original age model.

Introduction

Hoyanagi et al. (2014) reported oxygen and stable carbon isotope ratios of the benthic foraminifer *Nanionella flemingi* in cores from Hole U1352B, which was drilled on the upper slope offshore Canterbury Basin (New Zealand) during Integrated Ocean Drilling Program (IODP) Expedition 317. The oxygen isotope record was correlated with the LR04 stack (Lisiecki and Raymo, 2005) with the support of shipboard bioevent ages (see the “Site U1352” chapter [Expedition 317 Scientists, 2011b]) to generate an age model for the upper 500 m of Hole U1352B.

Although the nannofossil bioevent highest occurrence (HO) of *Pseudoemiliania lacunosa* (0.44 Ma) was used for the age model in **Hoyanagi et al.** (2014), the following problems have since been identified:

- *Pseudoemiliania ovata* and *Pseudoemiliania pacifica* were found above the HO of *P. lacunosa* datum (see the “Site U1352” chapter [Expedition 317 Scientists, 2011b]).
- The benthic foraminiferal bioevent, HO of *Bolivinita pliozea* (0.6 Ma), was placed above the HO of *P. lacunosa* (0.44 Ma) in Hole U1352B (i.e., the older age datum was placed above the



younger age datum). Such a depth reversal for these two bioevent datums was also recognized in Holes U1351B and U1354B.

- The HO of *P. lacunosa* defines the nannofossil Zone NN20/NN19 boundary and coincides with marine isotope Stage (MIS) 12. However, [Hoyanagi et al.](#) (2014) did not find a significant positive oxygen isotopic peak, which would be expected at MIS 12, near the core position originally chosen for the HO of *P. lacunosa* during Expedition 317 (i.e., between 155.99 and 164.18 m; all depths are core depth below seafloor, Method A [CSF-A]) (see the “[Site U1352](#)” chapter [Expedition 317 Scientists, 2011b]). [Hoyanagi et al.](#) (2014) measured oxygen and carbon isotopes every ~1.5 m in this interval, resulting in samples <5500 y apart, assuming an average sedimentation rate of 28 cm/1000 y (see below). Therefore, we should be able to recognize $\delta^{18}\text{O}$ and $\delta^{13}\text{C}$ fluctuations with cycle periods exceeding 11,000 y, which is sufficient to resolve MISs.

Sea level is considered to have risen 135 m from glacial MIS 12 to interglacial MIS 11 (Miller et al., 2005), so the absence of a positive oxygen isotopic ratio peak at the Zone NN20/NN19 boundary in the [Hoyanagi et al.](#) (2014) age model is troubling. Therefore, we have reexamined the occurrence of *P. lacunosa* and have made additional isotopic measurements of benthic foraminifer *N. flemingi* in Hole U1352B cores. These new data indicate that the shipboard depth of the HO of *P. lacunosa* should be revised for the following reasons.

Genus *Pseudoemiliania* was divided into two species, *P. lacunosa* and *P. ovata*, by Young (1998). Specimens of *P. ovata* larger than 6.5 μm were further defined as *P. pacifica* by de Kaenel et al. (1999). Usually, the HO of *P. lacunosa* is defined by the last occurrences of the genus *Pseudoemiliania* (i.e., any of these species), and the HO of *P. lacunosa* occurs in almost same horizon as the HO of *P. ovata* (Expedition 315 Scientists, 2009). Expedition 317 Scientists placed the HO of *P. lacunosa* at the horizon between 155.99 and 164.18 m. However, samples at 141.14 m yield *P. ovata* and *P. pacifica* in the cores from Hole U1352B (see the “[Site U1352](#)” chapter [Expedition 317 Scientists, 2011b]); the HO of *P. lacunosa* should therefore be no deeper than 141.14 m.

Reexamination of the depth of the HO of *P. lacunosa* in Hole U1352B and additional measurements of benthic foraminiferal oxygen and stable carbon isotope ratios presented in this report lead to a revised correlation with the LR04 stack and a new age model for Hole U1352B. Furthermore, [Hoyanagi et al.](#) (2014) did not evaluate the vital effect of *N. flemingi*. We therefore have conducted new measurements of

oxygen and stable carbon isotopic ratios of the benthic foraminifer *Uvigerina perigrina*, which occurs rarely in the cores, to ensure that correlation of isotopic measurements made on *N. flemingi* with the LR04 stack is justified.

Our new results suggest that the original age model ([Hoyanagi et al.](#), 2014) should be modified in the intervals between 115 and 215 m and between 255 and 305 m. The former age model is unchanged outside these intervals. All data presented in [Hoyanagi et al.](#) (2014) are duplicated in this report.

Materials and methods

We picked 36 samples for microscopic analysis of calcareous nannofossils every 0.83 to 4.52 m, with an average spacing of 1.5 m or one sample per section, from 180.4 to 122.37 m in Hole U1352B (Table T1) to determine the HO of *P. lacunosa* (Zone NN20/NN19).

Smear slides were examined under a polarized microscope at 1250 \times magnification. Three hundred calcareous nannofossils were identified to species level in each slide. The total abundance of calcareous nannofossils was defined as follows:

A = abundant; usually >10 specimens observed per field of view (FOV).

C = common; 1–10 specimens per FOV.

F = few; 1 specimen per FOV.

R = rare; 1 specimen per 1–10 FOVs.

VR = very rare; <1 specimen per 10 FOVs.

B = barren; no nannofossils.

Calcareous nannofossil preservation was recorded using the following criteria (see the “[Methods](#)” chapter [Expedition 317 Scientists, 2011a]):

M = moderate; some etching and/or recrystallization; primary morphological characteristics partially altered; most specimens identifiable at the species level.

P = poor; specimens severely etched or overgrown; primary morphological characteristics largely destroyed; fragmentation evident; most specimens not identifiable at the species and/or generic level.

Analyses of oxygen and stable carbon isotope ratios of benthic foraminifer *N. flemingi* were carried out on 23 samples from 62–68 m, 8 samples from 95–100 m, 41 samples from 123–151 m, 20 samples from 197–202 m, 21 samples from 247–253 m, 22 samples from 426–432 m, and 42 samples from 446–456 m. A total of 177 samples were measured. The spacing between our new measurements ranges from a mini-

mum of 0.2 m to a maximum of 1.45 m and averages 0.5 m for 123–151 m, where the focus was on the HO of *P. lacunosa* and MIS 12 (Table T2). This 0.5 m sample interval represents ~3300 y.

Several *U. perigrina* tests were picked from each of 88 samples from Hole U1352B between 156.4 and 501 m. We measured their oxygen and carbon isotope ratios and compared the ratios with those of *N. flemingi* from the same horizons (Table T3).

Oxygen and stable carbon isotopic analyses were carried out at the Kochi Core Center using an IsoPrime mass spectrometer. We used the same sample preparation and analytical procedures as Hoyanagi et al. (2014). Analytical precision is better than 0.08‰ for $\delta^{18}\text{O}$ and 0.05‰ for $\delta^{13}\text{C}$.

Results

Nannofossil datum reexamination

Results of microscopic observation of nannofossil occurrences are shown in Table T1. *P. lacunosa* is found from 128.35 to 180.06 m. *P. ovata* is found from 130.34 to 159.47 m. *P. pacifica* was observed in two samples at 157.86 and 175.07 m (Table T1; Fig. F1). Therefore, we confirmed that the occurrences of *P. lacunosa* and/or *P. ovata* are as shallow as 131.98 m (Table T1). The isolated occurrence of *P. lacunosa* var. *lacunosa* at 128.35 m is considered to be reworked. Therefore, we propose that the HO of *P. lacunosa* (Zone NN20/NN19; 0.44 Ma) in Hole U1352B be placed between 129.77 and 130.34 m (Table T4).

Impact of new isotopic measurements

The measured interval between 123 and 151 m includes our revised depth of the HO of *P. lacunosa* (131.98 m). Oxygen isotope ratios were relatively high throughout this interval in Hoyanagi et al. (2014). In contrast, our new measurements resolve two additional positive peaks and one new negative excursion within this interval (Fig. F2). However, the new measurements reveal no new peaks outside this interval.

Although the average sedimentation rate in the upper 500 m of Hole U1352B is 28 cm/ky, a lower rate (17 cm/ky) is estimated for the interval between the HO of *P. lacunosa* and the lowest occurrence (LO) of *Emiliania huxleyi* (121.1 m). Hoyanagi et al. (2014) measured isotopic ratios at 1.5 m intervals. This interval represents ~5400 y with a sedimentation rate of 28 cm/ky but ~8800 y with a rate of 17 cm/ky. Hoyanagi et al. (2014) could therefore have missed several oxygen isotopic ratio peaks in the interval where the sedimentation rate is low. The addition of

41 new measurements in the key 123–151 m interval to the original 58 measurements of Hoyanagi et al. (2014) increases measurement resolution to ~3000 y with a 17 cm/ky sedimentation rate and led to resolution of the previously undetected peaks.

Comparison of oxygen and stable carbon isotopic ratios for *N. flemingi* and *U. perigrina* is shown in Figure F2. The oxygen isotope ratios of *N. flemingi* have a strong correlation with those of *U. perigrina* (Fig. F3). The relationship between oxygen isotopic ratios of *N. flemingi* (Y) and *U. perigrina* (X) is expressed by the equation $Y = X + 0.27$. Therefore, oxygen isotope ratios of *N. flemingi* and *U. perigrina* can essentially be used interchangeably. The stable carbon isotopic ratios of the two species also show a positive correlation (Fig. F4). Because *U. perigrina* is considered to have the same oxygen and stable carbon isotopic ratios as the surrounding seawater (Shackleton and Hall, 1984), *N. flemingi* must also have the same or very similar oxygen and carbon isotopic ratios as those of ambient seawater and can therefore be correlated with the LR04 stack, which is based on *U. perigrina*.

Correlation with the LR04 stack and revised age model

The HO of *P. lacunosa* marks the top of Zone NN19 (Martini, 1971) and the top of Subzone CN14a (Okada and Bukry, 1980). Previous studies have demonstrated the worldwide synchronicity of this datum, which corresponds to MIS 12 (e.g., Thierstein et al., 1977; Wei, 1993; Raffi et al., 2006). Our new oxygen isotope measurements show new positive peaks at ~130 m ($\delta^{18}\text{O} = 4.023\text{\textperthousand}$ at 129.90 m) and ~137 m ($\delta^{18}\text{O} = 3.825\text{\textperthousand}$ at 137.08 m) and a new negative peak at ~135 m ($\delta^{18}\text{O} = 3.059\text{\textperthousand}$ at 134.84 m) (Fig. F2; Table T2). Using our revised HO of *P. lacunosa* (0.44 Ma) at 131.98 m (Table T4), we correlate these new positive peaks with MIS 12 and 14 and the negative peak with MIS 13. Our new correlations show a clear positive peak in $\delta^{18}\text{O}$ at the HO of *P. lacunosa* that is concordant with the timescale of Lourens et al. (2004).

Expedition 317 Scientists suggested that a hiatus from 1.8 to 2.7 Ma lies somewhere between 491.74 and 525.34 m. Therefore, we use the eight Pleistocene nannofossil datum levels shallower than 491.74 m (Table T4; see the “Site U1352” chapter [Expedition 317 Scientists, 2011b]) to correlate the $\delta^{18}\text{O}$ record (Fig. F5A) with the global benthic foraminiferal $\delta^{18}\text{O}$ LR04 stack of Lisiecki and Raymo (2005) (Fig. F5B) and to plot the Expedition 317 $\delta^{18}\text{O}$ record versus age from 1.8 Ma to present.



We made revised correlations relative to [Hoyanagi et al. \(2014\)](#) for the intervals between MIS 11 and 17 and between MIS 25 and 29 (Fig. F5C). *N. flemingi* tests were present in the interval between 62 and 66 m but were not present between 10.7 and 62 m. Therefore, we cannot correlate our record to MIS 4 of the LR04 stack. Other correlations of [Hoyanagi et al. \(2014\)](#) between the Hole U1352B oxygen isotope record and the LR04 stack were left unchanged (Fig. F5).

Figure F6 shows the sedimentation rates (age model) for Hole U1352B. The ages within the intervals between 115 and 215 m and between 255 and 305 m are shifted relative to the ages in [Hoyanagi et al. \(2014\)](#). Maximum age differences between the two models is ~0.2 my for the same depth. The new age model (Fig. F6) indicates that the average sedimentation rate in the upper ~500 m of Hole U1352B is ~28 cm/1000 y. However, sedimentation rates fluctuate; the maximum rate is ~76 cm/1000 y between 0.8 and 0.7 Ma and the minimum rate is ~3 cm/1000 y between 0.9 and 0.8 Ma.

Acknowledgments

This research used samples and data provided by the Integrated Ocean Drilling Program (IODP). We acknowledge the IODP Expedition 317 shipboard scientists, technical staff, and the captain and crew of the R/V *JOIDES Resolution*. We would like to thank Clara T. Bolton and an anonymous reviewer. This article was greatly improved by their detailed review and valuable suggestions. Oxygen and stable carbon isotopic measurements were performed under the cooperative research program of the Center for Advanced Marine Core Research (CMCR), Kochi University (Numbers 13A034, 13B028, 14A031, 14B029, 15A039, and 15B034). Funding for this research was provided by Japan Society for the Promotion of Science (JSPS Grants-in Aid for Scientific Research Number 23340154).

References

- de Kaenel, E., Siesser, W.G., and Murat, A., 1999. Pleistocene calcareous nannofossil biostratigraphy and the western Mediterranean sapropels, Sites 974 to 977 and 979. In Zahn, R., Comas, M.C., and Klaus, A. (Eds.), *Proceedings of the Ocean Drilling Program, Scientific Results*, 161: College Station, TX (Ocean Drilling Program), 159–183. <https://doi.org/10.2973/odp.proc.sr.161.250.1999>
- Expedition 315 Scientists, 2009. Expedition 315 Site C0002. In Kinoshita, M., Tobin, H., Ashi, J., Kimura, G., Lallemand, S., Sreaton, E.J., Curewitz, D., Masago, H., Moe, K.T., and the Expedition 314/315/316 Scientists, *Proceedings of the Integrated Ocean Drilling Program*, 314/315/316: Washington, DC (Integrated Ocean Drilling Program Management International, Inc.). <https://doi.org/10.2204/iodp.proc.314315316.124.2009>
- Expedition 317 Scientists, 2011a. Methods. In Fulthorpe, C.S., Hoyanagi, K., Blum, P., and the Expedition 317 Scientists, *Proceedings of the Integrated Ocean Drilling Program*, 317: Tokyo (Integrated Ocean Drilling Program Management International, Inc.). <https://doi.org/10.2204/iodp.proc.317.102.2011>
- Expedition 317 Scientists, 2011b. Site U1352. In Fulthorpe, C.S., Hoyanagi, K., Blum, P., and the Expedition 317 Scientists, *Proceedings of the Integrated Ocean Drilling Program*, 317: Tokyo (Integrated Ocean Drilling Program Management International, Inc.). <https://doi.org/10.2204/iodp.proc.317.104.2011>
- Hoyanagi, K., Kawagata, S., Koto, S., Kamihashi, T., and Ichihara, M., 2014. Data report: Pleistocene benthic foraminiferal oxygen and stable carbon isotopes and their application for age models, Hole U1352, offshore New Zealand. In Fulthorpe, C.S., Hoyanagi, K., Blum, P., and the Expedition 317 Scientists, *Proceedings of the Integrated Ocean Drilling Program*, 317: Tokyo (Integrated Ocean Drilling Program Management International, Inc.). <https://doi.org/10.2204/iodp.proc.317.208.2014>
- Kameo, K., and Bralower, T.J., 2000. Neogene calcareous nannofossil biostratigraphy of Sites 998, 999, and 1000, Caribbean Sea. In Leckie, R.M., Sigurdsson, H., Acton, G.D., and Draper, G. (Eds.), *Proceedings of the Ocean Drilling Program, Scientific Results*, 165: College Station, TX (Ocean Drilling Program), 3–17. <https://doi.org/10.2973/odp.proc.sr.165.012.2000>
- Lisicki, L.E., and Raymo, M.E., 2005. A Pliocene–Pleistocene stack of 57 globally distributed benthic $\delta^{18}\text{O}$ records. *Paleoceanography*, 20(1):PA1003. <https://doi.org/10.1029/2004PA001071>
- Lourens, L., Hilgen, F., Shackleton, N.J., Laskar, J., and Wilson, D., 2004. The Neogene period. In Gradstein, F.M., Ogg, J.G., and Smith, A. (Eds.), *A Geologic Time Scale 2004*: Cambridge, UK (Cambridge Univ. Press), 409–440. <https://doi.org/10.1017/CBO9780511536045.022>
- Martini, E., 1971. Standard Tertiary and Quaternary calcareous nannoplankton zonation. In Farinacci, A. (Ed.), *Proceeding of the Second Planktonic Conference Roma 1970*: Rome (Edizioni Tecnoscienza), 2:739–785.
- Miller, K.G., Kominz, M.A., Browning, J.V., Wright, J.D., Mountain, G.S., Katz, M.E., Sugarman, P.J., Cramer, B.S., Christie-Blick, N., and Pekar, S.F., 2005. The Phanerozoic record of global sea-level change. *Science*, 310(5752):1293–1298. <https://doi.org/10.1126/science.1116412>
- Okada, H., and Bukry, D., 1980. Supplementary modification and introduction of code numbers to the low-latitude coccolith biostratigraphic zonation (Bukry, 1973; 1975). *Marine Micropaleontology*, 5:321–325. [https://doi.org/10.1016/0377-8398\(80\)90016-X](https://doi.org/10.1016/0377-8398(80)90016-X)
- Paillard, D., Labeyrie, L., and Yiou, P., 1996. Macintosh program performs time-series analysis. *Eos, Transactions of the American Geophysical Union*, 77(39):379. <https://doi.org/10.1029/96EO00259>



- Raffi, I., Backman, J., Fornaciari, E., Pälike, H., Rio, D., Lourens, L., and Hilgen, F., 2006. A review of calcareous nannofossil astrobiochronology encompassing the past 25 million years. *Quaternary Science Reviews*, 25(23–24):3113–3137. <https://doi.org/10.1016/j.quascirev.2006.07.007>
- Shackleton, N.J., and Hall, M.A., 1984. Oxygen and carbon isotope stratigraphy of Deep Sea Drilling Project Hole 552A: Plio–Pleistocene glacial history. In Roberts, D.G., Schnitker, D., et al., *Initial Reports of the Deep Sea Drilling Project*, 81: Washington, DC (U.S. Government Printing Office), 599–609. <https://doi.org/10.2973/dsdp.proc.81.116.1984>
- Thierstein, H.R., Geitzenauer, K.R., Molfino, B., and Shackleton, N.J., 1977. Global synchronicity of late Quaternary coccolith datum levels validation by oxygen isotopes. *Geology*, 5(7):400–404. [https://doi.org/10.1130/0091-7613\(1977\)5<400:GSOLQC>2.0.CO;2](https://doi.org/10.1130/0091-7613(1977)5<400:GSOLQC>2.0.CO;2)
- Young, J.R., 1998. Neogene. In Bown, P.R. (Ed.), *Calcareous Nannofossil Biostratigraphy*: Dordrecht, The Netherlands (Kluwer Academic Publishing), 225–265.
- Wei, W., 1993. Calibration of upper Pliocene–lower Pleistocene nannofossil events with oxygen isotope stratigraphy. *Paleoceanography*, 8(1):85–99. <https://doi.org/10.1029/92PA02504>

Initial receipt: 27 March 2016

Acceptance: 22 June 2018

Publication: 7 September 2018

MS 317-210



Figure F1. Selected calcareous nannofossil species, Hole U1352B. Scale bars = 3 μm . A, B. *Pseudodemilianica lacunosa* (Kamptner) Gartner (139.25 m CSF-A). C. *Pseudodemilianica ovata* (Bukry) Young (157.86 m CSF-A). D. *Gephyrocapsa oceanica* Kamptner (128.35 m CSF-A).

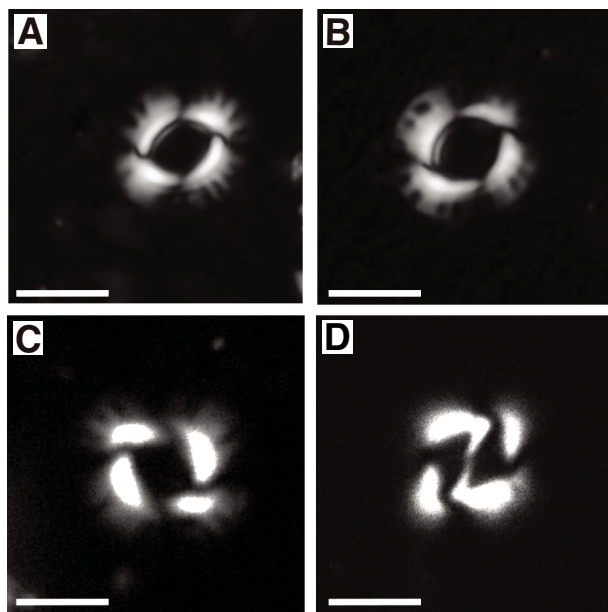


Figure F2. Oxygen and carbon isotope ratios of foraminifer *Nonionella flemingi* tests from 520 samples (solid lines), including data reported in Hoyanagi et al. (2014), and those of *Uvigerina perigrina* tests from 87 samples (dashed lines), Hole U1352B. Solid circles = measured values. Orange = $\delta^{13}\text{C}$, blue = $\delta^{18}\text{O}$. VPDB = Vienna PeeDee belemnite.

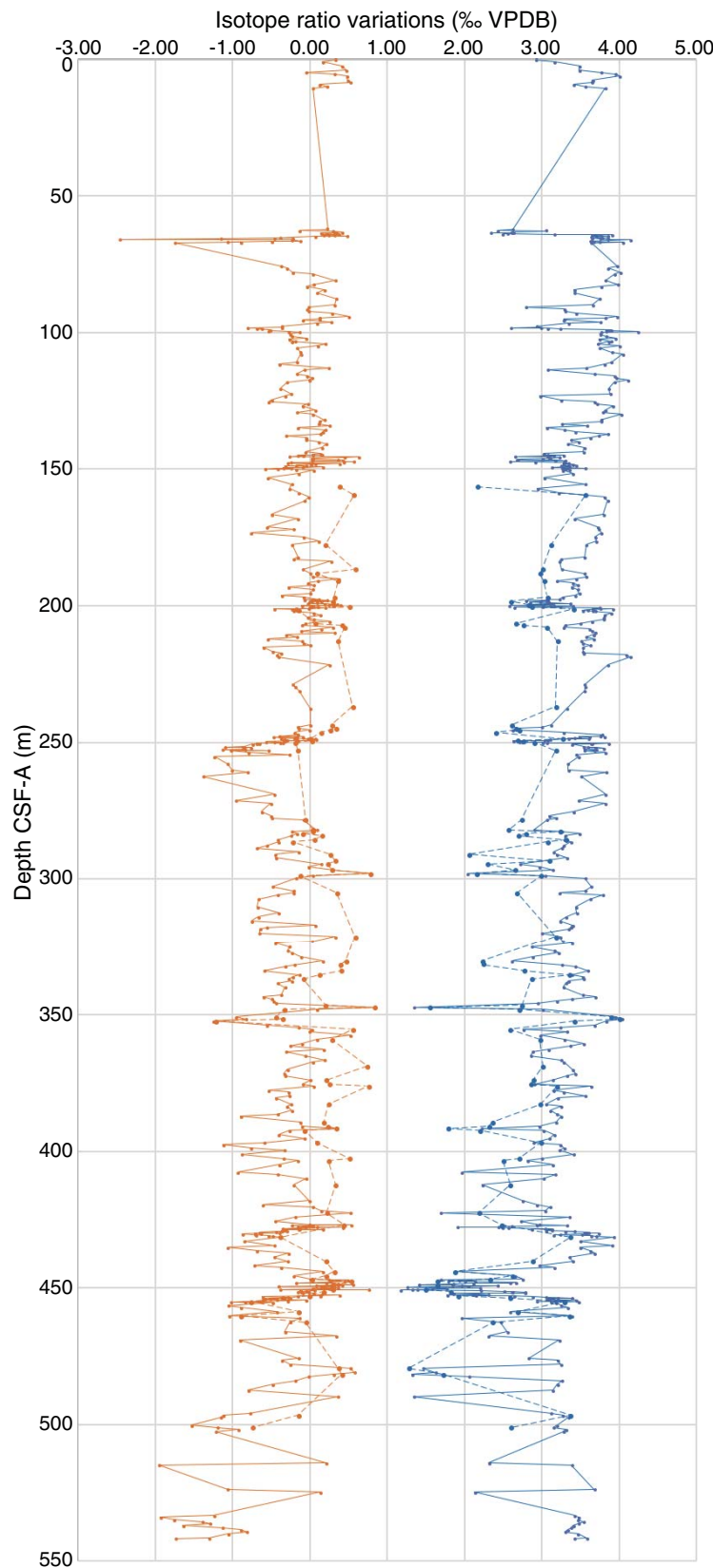


Figure F3. Comparison between oxygen isotopic measurements made on *Nonionella flemingi* and *Uvigerina peregrina*, Hole U1352B. All *N. flemingi* values, except that at 249.48 m CSF-A, are from Hoyanagi et al. (2014). VPDB = Vienna PeeDee belemnite.

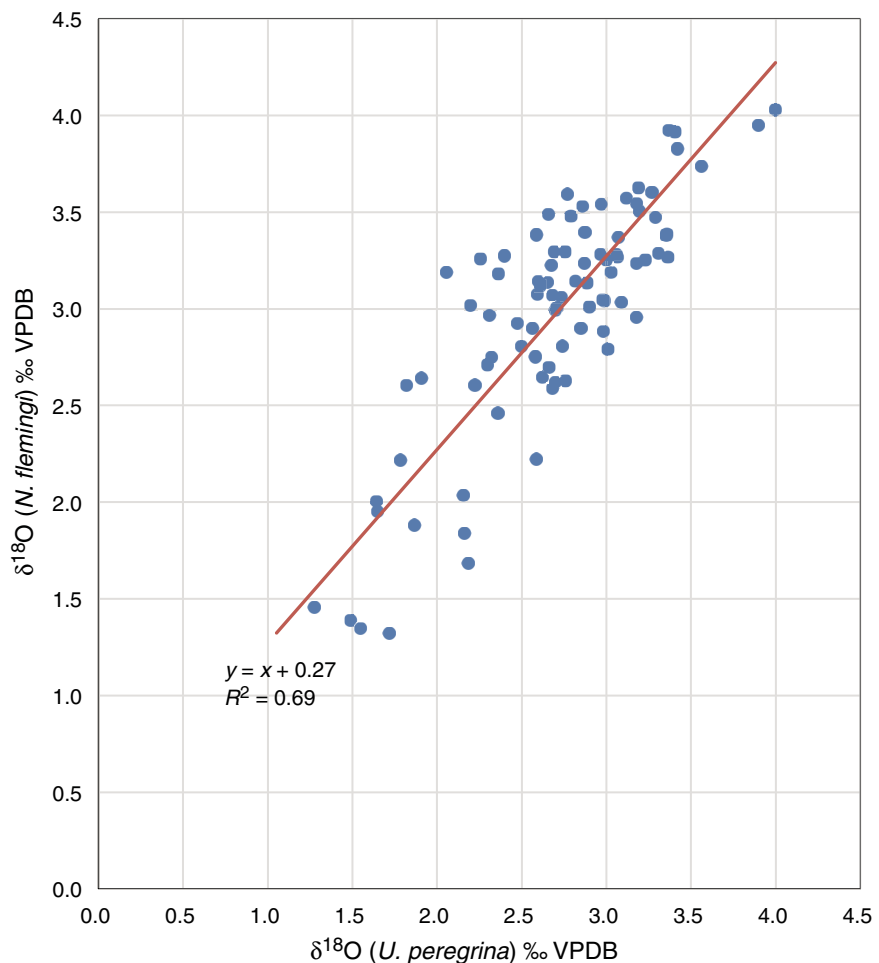


Figure F4. Comparison between carbon isotopic measurements made on *Nonionella flemingi* and *Uvigerina peregrina*, Hole U1352B. All *N. flemingi* values, except that at 249.48 m CSF-A, are from Hoyanagi et al. (2014). VPDB = Vienna Peepee belemnite.

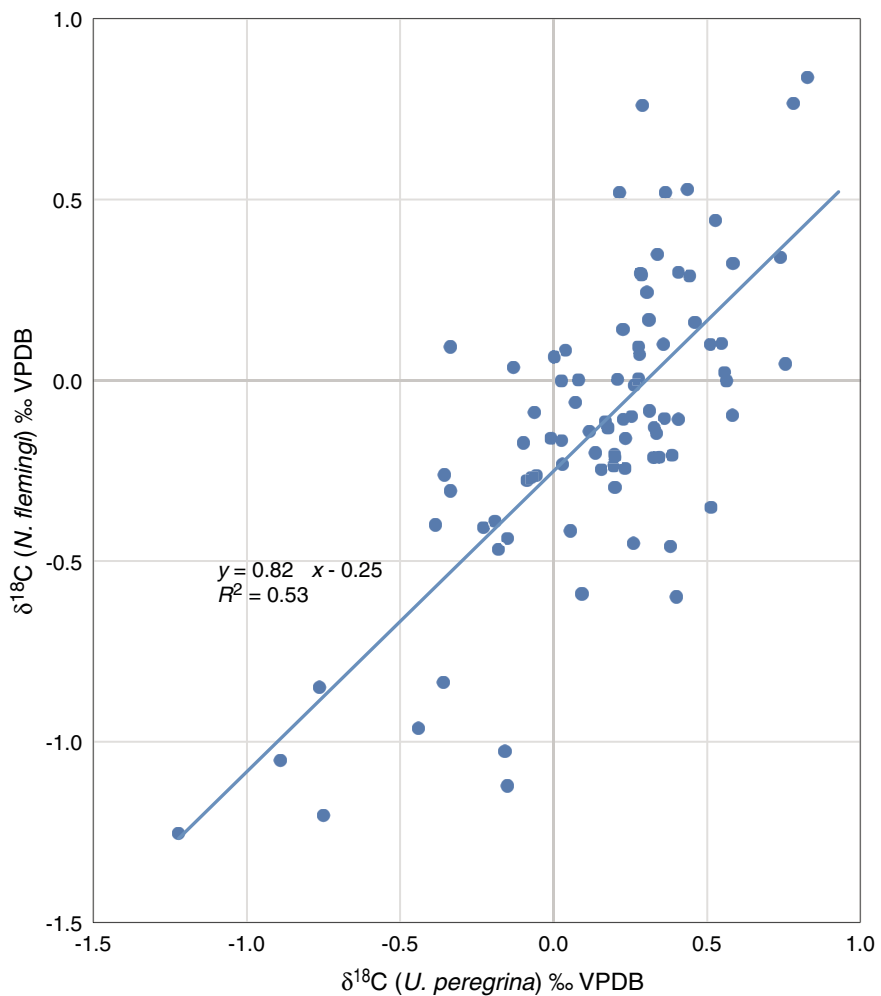


Figure F5. Oxygen isotope variations and LR04 stack (Lisiecki and Raymo, 2005), Site U1352. Numbers adjacent to data curves are marine isotope stages. A. 0–502 m CSF-A. Orange bars and lines = nannofossil datum ages (see Table T4). LO = lowest occurrence, HO = highest occurrence, HCO = highest common occurrence. Numbers in parentheses are ages (Ma). B. LR04 stack. C. Rescaled oxygen isotope variations (AnalySeries 2.0.4.3 software; Paillard et al., 1996) versus age. Red MIS numbers = correlations that are new and differ from those of [Hoyanagi et al. \(2014\)](#).

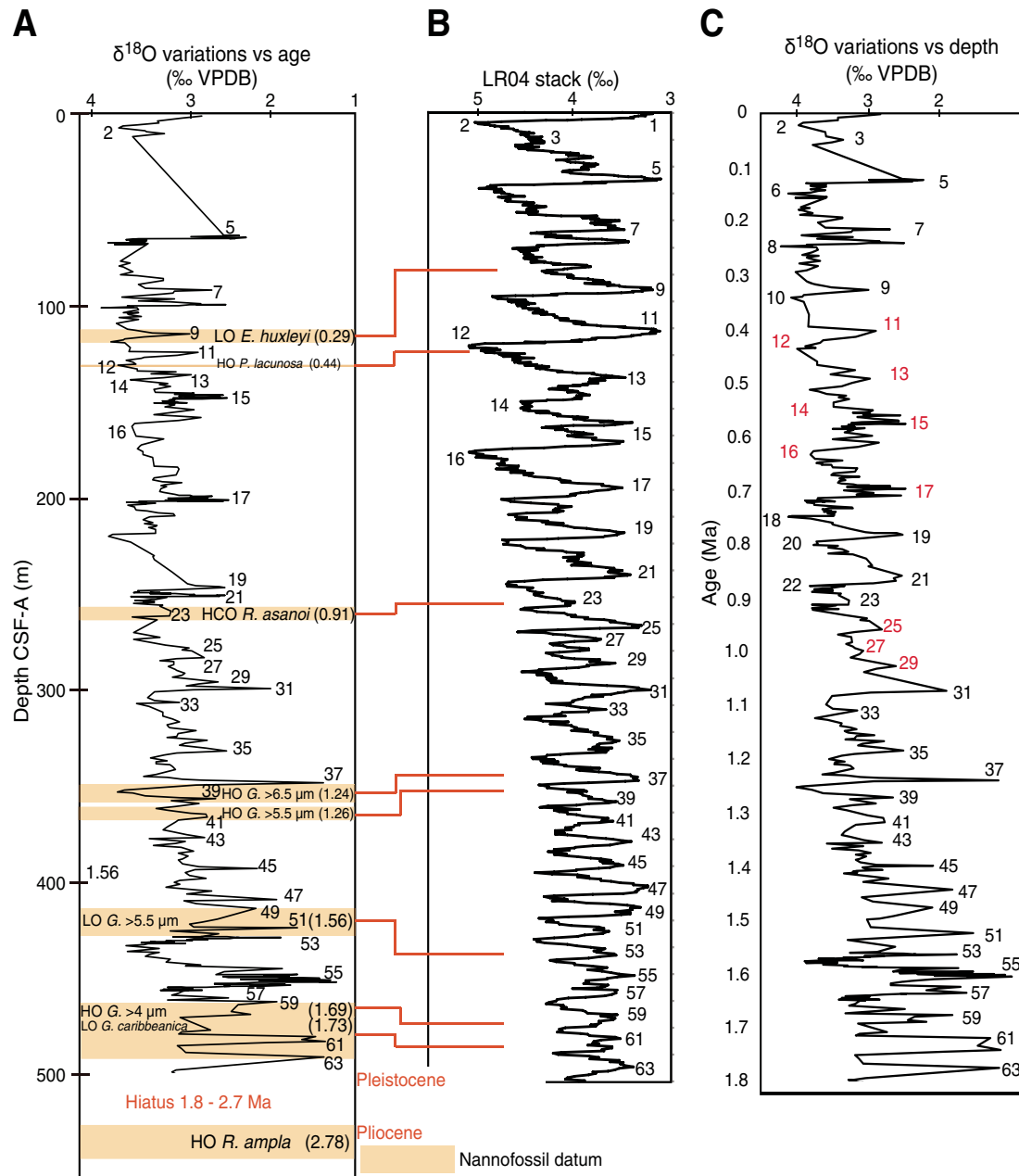


Figure F6. Sedimentation rates, Hole U1352B. Thick line = data produced using AnalySeries 2.0.4.3 software (Paillard et al., 1996), thin line = data from [Hoyanagi et al.](#) (2014), dotted line = average sedimentation rate for upper 500 m CSF-A.

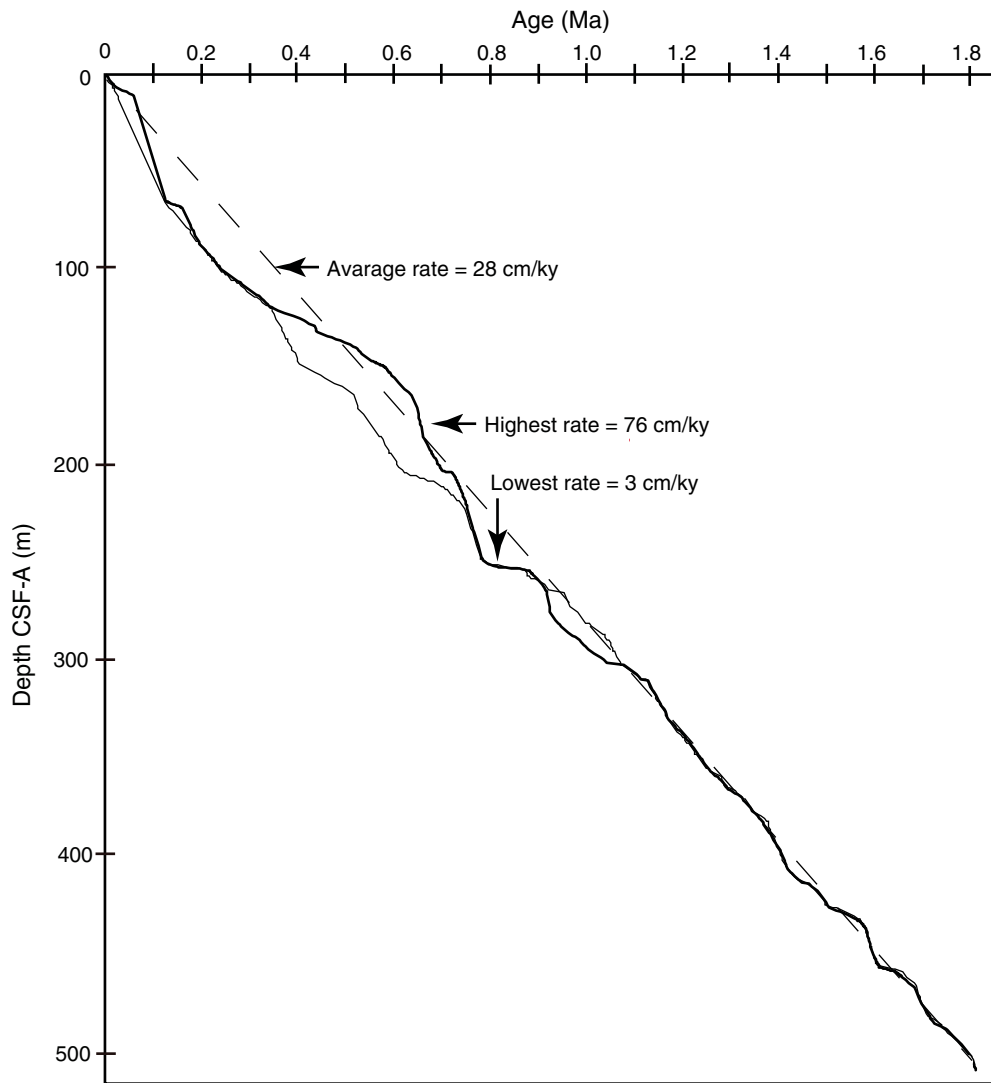


Table T1. Calcareous nannofossils, Hole U1352B.

Core, section, interval (cm)	Top depth (m)	Abundance/Preservation	<i>Calcidiscus leptopus</i>	<i>Coccolithus pelagicus</i>	<i>Coccolithus pelagicus f. braarudii</i>	<i>Coccolithus streekeri</i>	<i>Cyclcoccolithus floridanus</i>	<i>Dicyclocites antarcticus</i>	<i>Discoaster deflandrei</i>	<i>Discoaster sp.</i>	<i>Gephyrocapsa aperta</i>	<i>Gephyrocapsa caribbeanica</i> (3–4 µm)	<i>Gephyrocapsa caribbeanica</i> (4–5.5 µm)	<i>Gephyrocapsa oceanica</i> (3–4 µm)	<i>Gephyrocapsa oceanica</i> (4–5.5 µm)	<i>Helicosphaera carteri</i>	<i>Pseudoemiliania lacunosa</i>	<i>Pseudoemiliania ovata</i>	<i>Pseudoemiliania pacifica</i>	<i>Reticulofenestra gelida</i> (8–10 µm)	<i>Reticulofenestra haqii</i> (3–5 µm)	<i>Reticulofenestra minuta</i> (<3 µm)	<i>Reticulofenestra minutula</i>	<i>Sphaerolithus fossils</i>	<i>Syracospaera</i> spp.	Total
317-U1352A-																										
14H-1, 17–18	122.37	C/M	14	1							3	81	197	1											300	
14H-1, 100–101	123.20	C/M	26	7	1						15	85	157	2											300	
14H-3, 17–18	125.37	C/M	34	1	1						41	65	139	9	1										300	
14H-4, 16–17	126.86	C/M	1	24	4	1					19	95	151	2											300	
14H-5, 15–16	128.35	C/M	1	16	13	1					12	80	3	163	6	1									305	
14H-5, 90–91	129.10	C/M	2	15	28	5	1				22	41	185												300	
14H-6, 7–8	129.77	C/M	2	14	2	2	1				32	84	152	3											300	
14H-CC, 8–9	130.34	C/M	3	29	2	1					29	105	122		1										300	
15H-1, 28–29	131.98	A/M	18	1	2						20	56	175	5	1	P									300	
15H-2, 25–26	133.45	C/M	1	12	2						14	30	216	2											300	
15H-3, 25–26	134.88	F/M	22								1	22	73	170		2									300	
15H-5, 25–26	137.75	C/M	3	22	1						37	51	174												300	
15H-6, 25–26	139.25	C/M	30	5							47	63	145	1	4	1									300	
15H-6, 100–101	140.00	C/M	1	23							31	95	144		P	P									300	
16H-1, 132–133	142.52	C/M	1	37		3					43	107	104	1	1	P	1								300	
16H-2, 129–130	143.99	B																							—	
16H-3, 133–134	145.50	B																							—	
16H-4, 101–102	146.68	F/M	1	1	2						31	123	139	1	2	P	P								300	
16H-7, 24–25	150.28	A/M	20	5							17	35	216												300	
17H-2, 114–115	153.34	C/M	5								45	7	238	2	1	P	P								300	
18H-2, 16–17	157.86	A/M	2	37	2	2	1				75	28	139	5	P	4	1								300	
18H-3, 27–28	159.47	F/M	2	17	2						90	88	94	1	2										300	
18H-6, 35–36	162.45	R/P	3	174	8						54	8	27												300	
18H-7, 34–35	163.54	B																							—	
19H-1, 35–36	166.05	VR/P	27								183	24	60												300	
19H-2, 36–37	167.56	B																							—	
19H-3, 36–37	169.06	B																							—	
19H-4, 62–63	170.82	VR/P	6	132	9						48	18	72	12											300	
19H-5, 53–54	172.23	B																							—	
19H-6, 36–37	173.53	C/M	3	38	21						61	79	85	8											300	
20H-1, 37–38	175.07	C/M	4	3							99	22	144			4									300	
20H-2, 38–39	176.58	B																							—	
20H-3, 6–7	177.44	C/M	2	31	7	3					239	1	9	1	P				1	4	1	1		300		
20H-4, 6–7	178.94	C/M	39	7	1						179	18	28	9				2	10	6	1			300		
20H-4, 117–118	180.06	C/M	2	36	10	1					173	25	29	13	P					11				300		
21H-1, 70–71	180.40	C/M	18	10	2	1					182	17	37							32	1			300		

Abundance: A = abundant, C = common, F = few, R = rare, VR = very rare, P = present outside the count, B = barren (no nannofossils). Preservation: M = moderate, P = poor.



Table T2. Oxygen isotopic ratios ($\delta^{18}\text{O}$) and stable carbon isotopic ratios ($\delta^{13}\text{C}$) of *Nanionella flemingi* from this study (177 samples) and Hoyanagi et al. (2014) (shaded cells; 341 samples), Hole U1352B. (Continued on next seven pages.)

Core, section, interval(cm)	Top depth CSF-A (m)	Middle depth CSF-A (m)	Bottom depth CSF-A (m)	$\delta^{13}\text{C}$ (‰ VPDB)	$\delta^{18}\text{O}$ (‰ VPDB)
317-U1352B-					
1H-1, 19–21	0.10	0.20	0.30	0.320	2.918
1H-1, 94–96	0.85	0.95	1.05	0.161	3.161
1H-2, 94–186	2.35	2.45	2.55	0.407	3.484
1H-3, 94–96	3.85	3.95	4.05	0.469	3.480
1H-4, 19–21	4.60	4.70	4.80	-0.054	3.762
1H-4, 94–96	5.35	5.45	5.55	0.315	3.941
1H-5, 19–21	6.10	6.20	6.30	0.472	4.005
1H-6, 19–21	7.50	7.60	7.70	0.483	3.651
2H-1, 19–21	8.30	8.40	8.50	0.517	3.638
2H-1, 94–96	9.05	9.15	9.25	0.122	3.408
2H-2, 20–22	9.81	9.91	10.01	0.219	3.561
2H-2, 94–96	10.55	10.65	10.75	0.037	3.811
7H-5, 46–48	62.16	62.17	62.18	0.234	2.621
7H-5, 92–94	62.62	62.63	62.64	-0.136	2.423
7H-5, 115–117	62.85	62.86	62.87	0.292	3.062
7H-6, 5–7	63.25	63.26	63.27	0.408	2.603
7H-6, 19–21	63.30	63.40	63.50	0.332	2.625
7H-6, 25–27	63.45	63.46	63.47	0.318	2.339
7H-6, 45–47	63.65	63.66	63.67	0.14	2.551
7H-6, 71–73	63.91	63.92	63.93	0.218	2.487
7H-6, 85–87	64.05	64.06	64.07	0.367	3.153
7H-6, 94–96	64.05	64.15	64.25	0.233	3.751
7H-6, 104–106	64.24	64.25	64.26	0.172	3.907
7H-6, 123–125	64.43	64.44	64.45	0.316	3.638
7H-CC, 23–25	64.68	64.69	64.70	0.479	3.849
7H-CC, 38–40	64.83	64.84	64.85	0.061	3.636
8H-1, 5–7	65.25	65.26	65.27	-0.388	3.778
8H-1, 19–21	65.30	65.40	65.50	-0.229	3.847
8H-1, 25–27	65.45	65.46	65.47	-0.461	3.648
8H-1, 45–47	65.65	65.66	65.67	-1.157	3.747
8H-1, 68–70	65.88	65.89	65.90	-2.461	3.846
8H-1, 85–87	66.05	66.06	66.07	-0.239	4.139
8H-1, 134–136	66.54	66.55	66.56	-0.128	3.623
8H-1, 145–147	66.65	66.66	66.67	-0.5	3.662
8H-2, 20–22	66.81	66.91	67.01	-0.897	4.046
8H-2, 13–15	66.83	66.84	66.85	-1.065	3.745
8H-2, 35–37	67.05	67.06	67.07	-1.748	3.634
9H-1, 94–96	75.55	75.65	75.75	-0.373	3.973
9H-2, 19–21	76.30	76.40	76.50	-0.298	3.853
9H-3, 19–21	77.80	77.90	78.00	-0.228	4.007
9H-3, 94–96	78.55	78.65	78.75	0.030	3.939
9H-5, 19–21	80.80	80.90	81.00	0.321	3.818
9H-6, 18–20	82.29	82.39	82.49	0.044	3.980
9H-6, 92–94	83.03	83.13	83.23	-0.047	3.757
10H-1, 19–21	84.30	84.40	84.50	0.180	3.416
10H-2, 95–97	85.32	85.42	85.52	0.091	3.421
10H-4, 19–21	87.56	87.66	87.76	0.338	3.746
10H-5, 94–96	89.81	89.91	90.01	0.317	3.649
10H-6, 19–21	90.56	90.66	90.76	-0.021	2.788
10H-6, 94–96	91.31	91.41	91.51	-0.040	3.283
10H-7, 20–22	92.07	92.17	92.27	-0.024	3.299
10H-7, 94–96	92.81	92.91	93.01	0.279	3.434
11H-1, 51–53	94.12	94.22	94.32	0.498	3.964
11H-1, 94–96	94.55	94.65	94.75	0.119	3.819
11H-1, 142–144	95.12	95.13	95.14	0.124	3.284
11H-2, 16–18	95.27	95.37	95.47	-0.095	3.280
11H-2, 94–96	96.05	96.15	96.25	0.273	3.754
11H-2, 134–136	96.54	96.55	96.56	0.083	3.336
11H-3, 94–96	97.55	97.65	97.75	-0.368	2.927
11H-3, 136–138	98.06	98.07	98.08	-0.368	2.987
11H-4, 11–13	98.29	98.30	98.31	-0.814	2.599
11H-4, 22–24	98.31	98.41	98.51	-0.626	3.073
11H-4, 40–42	98.58	98.59	98.60	-0.696	3.229
11H-4, 80–82	98.98	98.99	99.00	-0.523	3.896
11H-4, 94–96	99.03	99.13	99.23	-0.517	3.862



Table T2 (continued). (Continued on next page.)

Core, section, interval(cm)	Top depth CSF-A (m)	Middle depth CSF-A (m)	Bottom depth CSF-A (m)	$\delta^{13}\text{C}$ (‰ VPDB)	$\delta^{18}\text{O}$ (‰ VPDB)
11H-4, 110–112	99.28	99.29	99.30	-0.539	3.826
11H-4, 142–144	99.60	99.61	99.62	-0.276	4.237
11H-5, 19–21	99.78	99.88	99.98	-0.142	3.766
11H-5, 94–96	100.53	100.63	100.73	-0.261	3.751
11H-6, 19–21	101.28	101.38	101.48	-0.236	3.827
11H-6, 94–96	102.03	102.13	102.23	-0.057	3.950
11H-7, 19–21	102.28	102.38	102.48	-0.274	3.738
11H-7, 92–94	103.01	103.11	103.21	-0.198	3.890
12H-1, 19–21	103.30	103.40	103.50	-0.236	3.864
12H-1, 94–96	104.05	104.15	104.25	0.198	3.718
12H-2, 19–21	104.80	104.90	105.00	0.097	3.996
12H-2, 94–96	105.55	105.65	105.75	-0.170	3.745
12H-3, 94–96	107.01	107.11	107.21	-0.128	3.899
12H-4, 19–21	107.76	107.86	107.96	-0.119	4.041
12H-6, 19–21	110.76	110.86	110.96	-0.174	3.897
12H-6, 94–96	111.51	111.61	111.71	-0.403	3.809
13H-1, 19–21	112.80	112.90	113.00	0.243	3.569
13H-1, 93–95	113.54	113.64	113.74	-0.073	3.072
13H-2, 94–96	115.03	115.13	115.23	-0.173	3.673
13H-3, 19–21	115.78	115.88	115.98	-0.042	3.934
13H-3, 94–96	116.53	116.63	116.73	0.023	3.953
13H-4, 19–21	117.28	117.38	117.48	-0.013	4.104
13H-4, 94–96	118.03	118.13	118.23	-0.299	3.930
13H-6, 19–21	120.28	120.38	120.48	-0.384	3.860
14H-1, 19–21	122.30	122.40	122.50	-0.247	3.879
14H-1, 94–96	123.14	123.15	123.16	-0.323	2.973
14H-2, 94–96	124.64	124.65	124.66	-0.501	3.239
14H-3, 19–21	125.39	125.40	125.41	-0.54	3.677
14H-3, 94–96	126.05	126.15	126.25	-0.037	3.712
14H-4, 19–21	126.80	126.90	127.00	-0.102	3.915
14H-5, 19–21	128.30	128.40	128.50	0.060	3.819
14H-5, 94–96	129.05	129.15	129.25	-0.168	3.779
14H-6, 19–21	129.80	129.90	130.00	0.034	4.023
15H-1, 19–21	131.80	131.90	132.00	0.179	3.757
15H-1, 84–86	132.45	132.55	132.65	0.123	3.757
15H-2, 19–21	133.39	133.40	133.41	0.11	3.254
15H-2, 89–91	134.00	134.10	134.20	0.251	3.578
15H-3, 19–21	134.82	134.83	134.84	-0.162	3.059
15H-3, 94–96	135.57	135.58	135.59	0.192	3.287
15H-4, 19–21	136.32	136.33	136.34	0.163	3.429
15H-4, 94–96	136.98	137.08	137.18	0.129	3.852
15H-5, 19–21	137.60	137.70	137.80	-0.312	3.733
15H-5, 94–96	138.44	138.45	138.46	-0.052	3.624
15H-6, 19–21	139.19	139.20	139.21	-0.058	3.368
15H-6, 94–96	139.85	139.95	140.05	0.108	3.472
15H-7, 19–21	140.69	140.70	140.71	0.211	3.33
16H-1, 94–96	142.05	142.15	142.25	0.147	3.542
16H-2, 94–96	143.55	143.65	143.75	-0.060	3.534
16H-3, 14–16	144.31	144.32	144.33	0.125	3.019
16H-3, 34–36	144.51	144.52	144.53	0.032	3.032
16H-3, 54–56	144.71	144.72	144.73	0.154	3.065
16H-3, 74–76	144.91	144.92	144.93	-0.161	3.279
16H-3, 94–96	145.02	145.12	145.22	-0.086	3.143
16H-3, 91–93	145.08	145.09	145.1	-0.092	3.058
16H-3, 114–116	145.31	145.32	145.33	-0.265	2.647
16H-3, 134–136	145.51	145.52	145.53	0.627	3.086
16H-4, 4–6	145.71	145.72	145.73	0.438	3.226
16H-4, 24–26	145.91	145.92	145.93	0.035	3.107
16H-4, 44–46	146.11	146.12	146.13	0.017	3.007
16H-4, 67–69	146.34	146.35	146.36	0.038	2.683
16H-4, 84–86	146.51	146.52	146.53	0.362	2.674
16H-4, 107–109	146.74	146.75	146.76	0.421	3.168
16H-4, 120–122	146.87	146.88	146.89	0.018	3.3
16H-4, 144–146	147.11	147.12	147.13	0.559	2.58
16H-5, 14–16	147.31	147.32	147.33	0.429	2.912
16H-5, 34–36	147.51	147.52	147.53	-0.246	3.277
16H-5, 54–56	147.71	147.72	147.73	-0.296	3.343
16H-5, 75–77	147.92	147.93	147.94	0.376	3.279
16H-5, 91–93	148.08	148.09	148.10	0.069	3.274

Table T2 (continued). (Continued on next page.)

Core, section, interval(cm)	Top depth CSF-A (m)	Middle depth CSF-A (m)	Bottom depth CSF-A (m)	$\delta^{13}\text{C}$ (‰ VPDB)	$\delta^{18}\text{O}$ (‰ VPDB)
16H-5, 114–116	148.31	148.32	148.33	0.008	3.392
16H-5, 134–136	148.51	148.52	148.53	-0.182	3.434
16H-6, 4–6	148.71	148.72	148.73	-0.057	3.248
16H-6, 24–26	148.91	148.92	148.93	-0.329	3.352
16H-6, 44–46	149.11	149.12	149.13	0.167	3.338
16H-6, 60–62	149.27	149.28	149.29	-0.094	3.12
16H-6, 84–86	149.51	149.52	149.53	-0.347	3.258
16H-6, 93–95	149.51	149.61	149.71	-0.251	3.553
16H-6, 107–109	149.74	149.75	149.76	-0.426	3.279
16H-6, 128–130	149.95	149.96	149.97	-0.584	3.307
16H-7, 7–9	150.11	150.12	150.13	-0.189	3.347
16H-7, 27–29	150.31	150.32	150.33	0.042	3.269
17H-1, 93–95	151.54	151.64	151.74	-0.147	3.395
17H-2, 94–96	153.05	153.15	153.25	-0.550	3.022
17H-4, 90–92	155.30	155.40	155.50	-0.238	3.553
18H-1, 94–96	157.05	157.15	157.25	-0.269	2.937
18H-2, 92–94	158.53	158.63	158.73	-0.148	3.216
18H-3, 93–95	160.04	160.14	160.24	-0.017	3.801
18H-5, 94–96	161.45	161.55	161.65	-0.073	3.844
19H-1, 95–97	166.56	166.66	166.76	-0.501	3.790
19H-2, 94–96	168.05	168.15	168.25	-0.165	3.418
19H-4, 94–96	171.05	171.15	171.25	-0.558	3.715
19H-5, 19–21	171.80	171.90	172.00	-0.216	3.730
19H-6, 19–21	173.27	173.37	173.47	-0.767	3.766
20H-1, 19–21	174.80	174.90	175.00	-0.087	3.686
20H-2, 19–21	176.30	176.40	176.50	0.113	3.698
20H-3, 19–21	177.48	177.58	177.68	-0.237	3.573
21H-2, 94–96	182.05	182.15	182.25	-0.161	3.547
21H-3, 19–21	182.80	182.90	183.00	-0.220	3.242
21H-3, 94–96	183.55	183.65	183.75	0.269	3.224
21H-5, 94–96	186.55	186.65	186.75	-0.097	3.252
21H-6, 94–96	188.05	188.15	188.25	0.001	3.542
22H-1, 19–21	189.30	189.40	189.50	0.032	3.568
22H-1, 94–96	190.05	190.15	190.25	0.371	3.437
22H-2, 19–21	190.80	190.90	191.00	0.101	3.189
22H-2, 94–96	191.55	191.65	191.75	-0.027	3.399
22H-3, 19–21	192.30	192.40	192.50	0.040	3.464
22H-3, 93–95	193.04	193.14	193.24	-0.281	3.379
22H-4, 19–21	193.80	193.90	194.00	0.036	3.457
22H-5, 19–21	195.30	195.40	195.50	-0.003	3.476
22H-5, 95–97	196.06	196.16	196.26	-0.371	3.427
22H-6, 19–21	196.80	196.90	197.00	-0.085	3.270
22H-6, 94–96	197.55	197.65	197.75	0.105	3.219
22H-6, 98–100	197.68	197.69	197.70	-0.071	3.069
22H-6, 118–120	197.88	197.89	197.90	0.215	3.048
22H-6, 136–138	198.06	198.07	198.08	0.018	2.787
22H-7, 9–11	198.29	198.30	198.31	-0.008	3.058
22H-7, 19–21	198.30	198.40	198.50	0.292	3.076
22H-7, 31–33	198.51	198.52	198.53	0.139	2.973
22H-7, 49–51	198.69	198.70	198.71	0.083	2.838
23H-1, 37–39	199.07	199.08	199.09	-0.03	3.362
23H-1, 57–59	199.27	199.28	199.29	0.183	3.099
23H-1, 78–80	199.48	199.49	199.50	0.346	2.837
23H-1, 94–96	199.55	199.65	199.75	0.243	3.145
23H-1, 97–99	199.67	199.68	199.69	0.384	3.009
23H-1, 122–124	199.92	199.93	199.94	-0.112	2.578
23H-1, 137–139	200.07	200.08	200.09	0.03	3.4
23H-2, 9–11	200.29	200.30	200.31	0.02	3.001
23H-2, 19–21	200.30	200.40	200.50	0.099	3.235
23H-2, 32–34	200.52	200.53	200.54	-0.01	2.64
23H-2, 52–54	200.72	200.73	200.74	0.197	3.745
23H-2, 69–71	200.89	200.90	200.91	-0.019	3.754
23H-2, 94–96	201.05	201.15	201.25	-0.468	3.916
23H-2, 86–88	201.06	201.07	201.08	-0.241	3.651
23H-2, 129–131	201.49	201.50	201.51	-0.138	3.593
23H-2, 147–149	201.67	201.68	201.69	-0.162	3.522
23H-3, 19–21	201.80	201.90	202.00	-0.141	3.690
23H-3, 22–24	201.92	201.93	201.94	-0.215	3.652
23H-3, 94–96	202.55	202.65	202.75	0.039	3.893



Table T2 (continued). (Continued on next page.)

Core, section, interval(cm)	Top depth CSF-A (m)	Middle depth CSF-A (m)	Bottom depth CSF-A (m)	$\delta^{13}\text{C}$ (‰ VPDB)	$\delta^{18}\text{O}$ (‰ VPDB)
23H-4, 19–21	203.30	203.40	203.50	0.131	3.808
23H-4, 95–97	204.06	204.16	204.26	-0.028	3.798
23H-5, 19–21	204.80	204.90	205.00	0.041	3.791
23H-5, 94–96	205.55	205.65	205.75	0.245	3.644
23H-6, 19–21	206.30	206.40	206.50	-0.061	3.489
23H-6, 94–96	207.05	207.15	207.25	-0.107	3.295
23H-7, 19–21	207.80	207.90	208.00	0.289	3.281
24H-1, 19–21	208.30	208.40	208.50	0.144	3.609
24H-1, 94–96	209.05	209.15	209.25	-0.124	3.646
24H-2, 19–21	209.80	209.90	210.00	0.317	3.687
24H-2, 93–95	210.54	210.64	210.74	-0.313	3.663
24H-3, 19–21	211.30	211.40	211.50	-0.171	3.568
24H-3, 94–96	212.05	212.15	212.25	-0.546	3.670
24H-4, 19–21	212.80	212.90	213.00	-0.106	3.506
24H-4, 94–96	213.55	213.65	213.75	-0.089	3.522
24H-5, 18–20	214.29	214.39	214.49	0.005	3.619
24H-5, 94–96	215.05	215.15	215.25	-0.608	3.529
24H-6, 94–96	216.55	216.65	216.75	-0.491	3.525
24H-7, 18–20	217.29	217.39	217.49	-0.382	3.537
25H-1, 19–21	217.80	217.90	218.00	-0.427	4.089
25H-1, 94–96	218.55	218.65	218.75	-0.411	4.138
25H-3, 94–96	221.55	221.65	221.75	0.248	3.849
26H-2, 19–21	228.72	228.82	228.92	-0.230	3.551
26H-2, 94–96	229.47	229.57	229.67	-0.196	3.558
26H-3, 95–97	230.98	231.08	231.18	-0.141	3.549
27H-1, 94–96	237.55	237.65	237.75	0.002	3.317
27H-5, 94–96	243.55	243.65	243.75	0.004	3.118
27H-6, 19–21	244.30	244.40	244.50	-0.165	2.999
27H-6, 64–66	244.75	244.85	244.95	-0.148	2.696
27H-7, 19–21	245.30	245.40	245.50	-0.013	2.619
28H-1, 19–21	246.30	246.40	246.50	-0.201	3.274
28H-1, 94–96	247.05	247.15	247.25	-0.160	3.768
28H-2, 4–6	247.67	247.68	247.69	-0.403	3.749
28H-2, 19–21	247.73	247.83	247.93	-0.173	3.810
28H-2, 23–25	247.86	247.87	247.88	-0.095	3.478
28H-2, 44–46	248.07	248.08	248.09	-0.479	3.609
28H-2, 68–70	248.31	248.32	248.33	-0.204	3.418
28H-2, 84–86	248.47	248.48	248.49	-0.38	3.339
28H-2, 94–96	248.48	248.58	248.68	0.065	3.603
28H-2, 102–104	248.65	248.66	248.67	-0.03	3.28
28H-2, 124–126	248.87	248.88	248.89	0.074	3.099
28H-3, 19–21	249.23	249.33	249.43	-0.306	3.070
28H-3, 15–17	249.28	249.29	249.30	0.019	3.027
28H-3, 34–36	249.47	249.48	249.49	-0.167	2.627
28H-3, 54–56	249.67	249.68	249.69	-0.572	2.738
28H-3, 73–75	249.86	249.87	249.88	-0.46	2.706
28H-3, 94–96	249.98	250.08	250.18	-0.390	3.011
28H-3, 97–99	250.10	250.11	250.12	-0.356	3.059
28H-4, 17–19	250.21	250.31	250.41	-0.694	3.856
28H-4, 14–16	250.27	250.28	250.29	-0.694	3.628
28H-4, 33–35	250.46	250.47	250.48	-0.662	3.638
28H-4, 51–53	250.64	250.65	250.66	-0.749	3.387
29H-1, 27–29	251.47	251.48	251.49	-0.852	3.538
29H-1, 47–49	251.67	251.68	251.69	-1.103	3.592
29H-1, 69–71	251.90	251.91	251.92	-0.771	3.687
29H-1, 94–96	252.05	252.15	252.25	-0.875	3.796
29H-1, 129–131	252.49	252.50	252.51	-0.843	3.545
29H-1, 146–148	252.66	252.67	252.68	-1.13	3.694
29H-2, 19–21	252.80	252.90	253.00	-1.025	3.544
29H-2, 15–17	252.85	252.86	252.87	-0.539	3.678
29H-2, 94–96	253.55	253.65	253.75	-0.802	3.821
29H-3, 19–21	254.30	254.40	254.50	-0.268	3.441
29H-3, 94–96	255.05	255.15	255.25	-1.241	3.472
30H-1, 17–19	257.78	257.88	257.98	-1.066	3.333
30H-2, 94–96	260.05	260.15	260.25	-1.011	3.340
30H-3, 19–21	260.80	260.90	261.00	-0.808	3.828
30H-4, 18–20	262.29	262.39	262.49	-1.389	3.506
31H-2, 19–21	268.80	268.90	269.00	-0.462	3.821
31H-5, 18–20	271.10	271.20	271.30	-0.963	3.470



Table T2 (continued). (Continued on next page.)

Core, section, interval(cm)	Top depth CSF-A (m)	Middle depth CSF-A (m)	Bottom depth CSF-A (m)	$\delta^{13}\text{C}$ (‰ VPDB)	$\delta^{18}\text{O}$ (‰ VPDB)
32H-1, 19–22	272.31	272.41	272.51	-0.512	3.815
32H-3, 19–21	275.30	275.40	275.50	-0.628	3.404
32H-4, 19–21	276.80	276.90	277.00	-0.503	3.091
32H-4, 94–96	277.55	277.65	277.75	-0.500	3.183
32H-5, 19–21	278.25	278.35	278.45	-0.089	3.061
33H-1, 19–21	281.80	281.90	282.00	0.083	2.897
33H-1, 93–95	282.54	282.64	282.74	-0.233	3.254
33H-2, 19–21	283.21	283.31	283.41	-0.172	3.481
33H-3, 19–21	283.98	284.08	284.18	-0.248	3.297
33H-4, 94–96	285.49	285.59	285.69	-0.416	3.287
33H-5, 19–21	286.24	286.34	286.44	-0.407	3.371
33H-6, 19–21	287.72	287.82	287.92	-0.563	3.280
34H-2, 19–21	288.56	288.66	288.76	-0.693	3.252
34H-3, 18–20	289.98	290.08	290.18	-0.147	3.147
34H-4, 23–25	290.91	291.01	291.11	-0.450	3.188
34H-5, 97–99	292.02	292.12	292.22	-0.448	3.314
35H-2, 19–21	294.44	294.54	294.64	0.140	2.710
36H-1, 19–21	295.40	295.50	295.60	-0.023	2.966
36H-2, 19–21	296.60	296.70	296.80	0.296	3.137
37X-1, 94–96	297.85	297.95	298.05	0.767	2.035
37X-2, 19–21	298.60	298.70	298.80	0.035	3.043
37X-CC, 19–21	299.65	299.75	299.85	-0.184	3.556
38X-1, 19–21	302.70	302.80	302.90	-0.487	3.635
38X-2, 19–21	304.20	304.30	304.40	-0.217	3.553
38X-2, 94–96	304.95	305.05	305.15	-0.212	3.223
38X-3, 19–21	305.70	305.80	305.90	-0.426	3.782
38X-4, 19–21	307.20	307.30	307.40	-0.666	3.616
38X-6, 19–21	310.20	310.30	310.40	-0.683	3.434
39X-1, 19–21	312.30	312.40	312.50	-0.407	3.446
39X-2, 19–21	313.80	313.90	314.00	-0.673	3.313
39X-3, 19–21	315.30	315.40	315.50	-0.760	3.229
39X-4, 19–21	316.80	316.90	317.00	0.066	3.390
39X-4, 94–96	317.55	317.65	317.75	-0.563	3.368
39X-5, 19–21	318.30	318.40	318.50	-0.652	3.341
39X-6, 19–21	319.80	319.90	320.00	-0.656	2.999
39X-7, 19–21	321.10	321.20	321.30	0.323	3.235
40X-1, 94–96	322.75	322.85	322.95	0.022	3.261
40X-2, 19–21	323.50	323.60	323.70	-0.450	3.383
40X-3, 19–21	325.00	325.10	325.20	-0.275	2.864
40X-4, 19–21	326.50	326.60	326.70	-0.286	3.156
40X-4, 94–96	327.25	327.35	327.45	-0.243	3.215
40X-5, 94–96	328.75	328.85	328.95	-0.119	2.880
40X-6, 94–96	330.25	330.35	330.45	0.161	2.607
41X-1, 19–21	331.60	331.70	331.80	-0.207	3.258
41X-1, 94–96	332.35	332.45	332.55	-0.328	3.429
41X-2, 94–96	333.85	333.95	334.05	-0.600	3.595
41X-3, 94–96	335.35	335.45	335.55	-0.141	3.389
41X-4, 19–21	336.10	336.20	336.30	-0.222	3.521
41X-4, 94–96	336.85	336.95	337.05	-0.278	3.530
41X-5, 19–21	337.60	337.70	337.80	-0.239	3.346
41X-5, 94–96	338.35	338.45	338.55	-0.423	3.308
41X-6, 94–96	339.85	339.95	340.05	-0.326	3.273
42X-2, 19–21	342.70	342.80	342.90	-0.377	3.524
42X-2, 94–96	343.45	343.55	343.65	-0.610	3.690
42X-3, 19–21	344.20	344.30	344.40	-0.501	3.385
42X-3, 94–96	344.95	345.05	345.15	-0.472	3.187
42X-4, 19–21	345.70	345.80	345.90	-0.439	2.940
42X-5, 18–20	347.19	347.29	347.39	0.837	1.345
42X-5, 94–96	347.95	348.05	348.15	0.092	3.008
43X-1, 20–22	350.81	350.91	351.01	-0.962	3.950
43X-1, 95–97	351.56	351.66	351.76	-0.836	4.028
43X-2, 19–21	352.30	352.40	352.50	-1.254	3.828
43X-3, 19–21	353.80	353.90	354.00	-0.560	3.679
43X-3, 94–96	354.55	354.65	354.75	-0.152	3.230
43X-4, 19–21	355.30	355.40	355.50	0.021	2.753
43X-4, 94–96	356.05	356.15	356.25	-0.010	3.324
43X-5, 94–96	357.55	357.65	357.75	0.521	2.977
43X-6, 94–96	359.05	359.15	359.25	0.092	3.282
44X-1, 19–21	360.50	360.60	360.70	-0.106	3.535



Table T2 (continued). (Continued on next page.)

Core, section, interval(cm)	Top depth CSF-A (m)	Middle depth CSF-A (m)	Bottom depth CSF-A (m)	$\delta^{13}\text{C}$ (‰ VPDB)	$\delta^{18}\text{O}$ (‰ VPDB)
44X-1, 94–96	361.25	361.35	361.45	-0.257	3.365
44X-2, 94–96	362.75	362.85	362.95	0.178	3.081
44X-3, 19–21	363.50	363.60	363.70	-0.312	2.876
44X-4, 19–21	365.00	365.10	365.20	-0.060	2.854
44X-5, 19–21	366.50	366.60	366.70	0.189	3.239
44X-5, 94–96	367.25	367.35	367.45	0.036	3.281
45X-1, 19–21	370.10	370.20	370.30	-0.296	3.392
45X-2, 19–21	371.60	371.70	371.80	-0.340	3.432
45X-2, 94–96	372.35	372.45	372.55	-0.319	3.318
45X-3, 94–96	373.85	373.95	374.05	0.002	3.134
45X-4, 94–96	375.35	375.45	375.55	-0.100	2.899
45X-5, 19–21	376.10	376.20	376.30	0.045	3.628
45X-6, 19–21	377.60	377.70	377.80	-0.540	3.141
45X-6, 94–96	378.35	378.45	378.55	-0.279	3.272
46X-1, 19–21	379.70	379.80	379.90	-0.274	3.560
46X-1, 94–96	380.45	380.55	380.65	-0.446	3.204
46X-3, 19–21	382.68	382.78	382.88	-0.243	3.046
46X-3, 94–96	383.43	383.53	383.63	-0.302	3.247
46X-4, 94–96	384.93	385.03	385.13	-0.240	3.106
46X-5, 94–96	386.43	386.53	386.63	-0.426	3.193
46X-6, 19–21	387.18	387.28	387.38	-0.900	3.245
47X-1, 18–20	389.29	389.39	389.49	-0.132	3.183
47X-2, 19–21	390.80	390.90	391.00	-0.108	2.967
47X-2, 93–95	391.54	391.64	391.74	0.349	2.217
47X-3, 19–21	392.30	392.40	392.50	-0.269	3.018
47X-4, 18–20	393.79	393.89	393.99	-0.406	3.156
47X-5, 18–20	395.29	395.39	395.49	-0.074	3.096
47X-6, 18–20	396.79	396.89	396.99	-0.591	2.883
47X-6, 93–95	397.54	397.64	397.74	-1.125	3.230
48X-1, 19–21	398.80	398.90	399.00	-0.772	3.286
48X-1, 94–96	399.55	399.65	399.75	-0.331	3.223
48X-2, 94–96	401.05	401.15	401.25	-0.882	3.401
48X-3, 94–96	402.55	402.65	402.75	-0.351	2.993
48X-4, 19–21	403.30	403.40	403.50	-0.161	2.806
48X-5, 19–21	404.80	404.90	405.00	-0.404	3.140
48X-7, 19–21	407.60	407.70	407.80	-0.936	1.957
49X-1, 19–21	408.40	408.50	408.60	-0.419	3.168
49X-2, 19–21	409.90	410.00	410.10	-0.059	3.013
49X-3, 93–95	412.14	412.24	412.34	-0.214	2.224
50X-1, 19–21	418.00	418.10	418.20	-0.012	2.741
50X-2, 19–21	419.50	419.60	419.70	-0.611	2.930
50X-2, 98–100	420.29	420.39	420.49	0.033	3.098
50X-3, 94–96	421.75	421.85	421.95	0.138	3.041
50X-4, 19–21	422.50	422.60	422.70	0.520	1.682
50X-5, 19–21	424.00	424.10	424.20	-0.195	3.348
50X-6, 19–21	425.50	425.60	425.70	-0.450	2.721
50X-7, 19–21	426.80	426.90	427.00	0.527	2.925
50X-7, 16–18	426.86	426.87	426.88	-0.012	2.957
50X-7, 38–40	427.08	427.09	427.10	-0.242	3.317
50X-CC, 1–3	427.35	427.36	427.37	0.031	2.603
51X-1, 6–8	427.56	427.57	427.58	-0.07	2.437
51X-1, 19–21	427.60	427.70	427.80	0.087	1.903
51X-1, 16–18	427.66	427.67	427.68	-0.157	2.474
51X-1, 37–39	427.87	427.88	427.89	0.418	2.487
51X-1, 57–59	428.07	428.08	428.09	-0.16	2.567
51X-1, 77–79	428.27	428.28	428.29	-0.359	3.036
51X-1, 95–97	428.36	428.46	428.56	-0.140	3.127
51X-1, 98–100	428.48	428.49	428.50	-0.152	2.862
51X-1, 117–119	428.67	428.68	428.69	0.158	3.125
51X-1, 137–139	428.87	428.88	428.89	-0.34	3.122
51X-2, 9–11	429.09	429.10	429.11	-0.368	3.051
51X-2, 25–27	429.25	429.26	429.27	-0.3	3.411
51X-2, 45–47	429.45	429.46	429.47	-0.445	3.296
51X-2, 67–69	429.67	429.68	429.69	-0.658	3.595
51X-2, 85–87	429.85	429.86	429.87	-0.395	3.542
51X-2, 95–97	429.86	429.96	430.06	-0.718	3.734
51X-2, 109–111	430.09	430.10	430.11	-0.637	3.567
51X-2, 129–131	430.29	430.30	430.31	-0.878	3.517
51X-2, 147–149	430.47	430.48	430.49	-0.709	3.228

Table T2 (continued). (Continued on next page.)

Core, section, interval(cm)	Top depth CSF-A (m)	Middle depth CSF-A (m)	Bottom depth CSF-A (m)	$\delta^{13}\text{C}$ (‰ VPDB)	$\delta^{18}\text{O}$ (‰ VPDB)
51X-3, 15–17	430.65	430.66	430.67	-0.704	3.147
51X-3, 38–40	430.88	430.89	430.90	-0.536	3.637
51X-3, 58–60	431.08	431.09	431.10	-0.486	3.695
51X-3, 95–97	431.36	431.46	431.56	-0.400	3.924
51X-4, 94–96	432.85	432.95	433.05	-0.852	3.489
51X-5, 95–97	434.36	434.46	434.56	-0.467	3.906
51X-6, 19–21	435.10	435.20	435.30	-1.066	3.488
51X-7, 19–21	436.30	436.40	436.50	-0.689	3.620
52X-1, 19–21	437.20	437.30	437.40	-0.286	3.679
52X-2, 19–21	438.70	438.80	438.90	-0.467	3.348
52X-3, 19–21	440.20	440.30	440.40	-0.296	3.397
52X-4, 19–21	441.70	441.80	441.90	-0.726	2.957
52X-4, 94–96	442.45	442.55	442.65	-0.380	3.157
52X-5, 93–95	443.94	444.04	444.14	0.167	1.882
52X-6, 94–96	445.45	445.55	445.65	-0.213	2.647
53X-1, 19–21	446.80	446.90	447.00	-0.001	2.749
53X-1, 26–28	446.96	446.97	446.98	0.235	1.683
53X-1, 46–48	447.16	447.17	447.18	0.485	1.925
53X-1, 72–74	447.42	447.43	447.44	0.263	2.127
53X-1, 95–97	447.56	447.66	447.76	0.442	2.004
53X-1, 91–93	447.61	447.62	447.63	0.256	1.786
53X-1, 131–133	448.01	448.02	448.03	0.201	2.66
53X-2, 2–4	448.22	448.23	448.24	-0.185	2.589
53X-2, 16–18	448.36	448.37	448.38	0.306	2.103
53X-2, 38–40	448.58	448.59	448.60	0.357	1.847
53X-2, 59–61	448.79	448.8	448.81	0.548	1.403
53X-2, 77–79	448.97	448.98	448.99	0.352	1.833
53X-2, 94–96	449.05	449.15	449.25	0.071	1.953
53X-2, 97–99	449.17	449.18	449.19	0.415	2.423
53X-2, 117–119	449.37	449.38	449.39	-0.413	2.04
53X-2, 137–139	449.57	449.58	449.59	0.319	1.632
53X-3, 8–10	449.78	449.79	449.80	0.139	1.252
53X-3, 27–29	449.97	449.98	449.99	0.356	2.191
53X-3, 46–48	450.16	450.17	450.18	0.03	1.583
53X-3, 68–70	450.38	450.39	450.40	0.264	1.767
53X-3, 94–96	450.55	450.65	450.75	0.760	1.388
53X-3, 87–89	450.57	450.58	450.59	-0.393	1.317
53X-3, 107–109	450.77	450.78	450.79	-0.127	1.172
53X-3, 132–134	451.02	451.03	451.04	0.053	2.2
53X-4, 4–6	451.24	451.25	451.26	-0.056	2.504
53X-4, 19–21	451.30	451.40	451.50	-0.115	2.605
53X-4, 22–24	451.42	451.43	451.44	-0.023	2.615
53X-4, 43–45	451.63	451.64	451.65	-0.165	2.778
53X-4, 61–63	451.81	451.82	451.83	-0.094	2.778
53X-4, 81–83	452.01	452.02	452.03	0.043	1.853
53X-4, 103–105	452.23	452.24	452.25	0.04	2.155
53X-4, 121–123	452.41	452.42	452.43	0.138	2.303
53X-4, 141–143	452.61	452.62	452.63	0.382	1.769
53X-5, 7–9	452.77	452.78	452.79	-0.021	2.145
53X-5, 19–21	452.80	452.90	453.00	-0.160	2.641
53X-5, 27–29	452.97	452.98	452.99	0.13	2.57
53X-5, 52–54	453.22	453.23	453.24	-0.618	2.88
53X-5, 71–73	453.41	453.42	453.43	-0.292	3.05
53X-5, 94–96	453.55	453.65	453.75	-0.262	3.383
53X-5, 97–99	453.67	453.68	453.69	-0.332	3.203
53X-5, 113–115	453.83	453.84	453.85	-0.521	3.055
53X-5, 131–133	454.01	454.02	454.03	-0.583	3.104
53X-6, 2–4	454.19	454.20	454.21	-0.429	3.152
53X-6, 15–17	454.32	454.33	454.34	-0.615	3.065
53X-6, 35–37	454.52	454.53	454.54	-0.052	3.434
53X-6, 59–61	454.76	454.77	454.78	-0.295	3.291
53X-6, 82–84	454.99	455.00	455.01	-0.655	2.93
53X-6, 95–97	455.03	455.13	455.23	-0.848	3.474
53X-6, 101–103	455.18	455.19	455.20	-1.026	3.109
53X-6, 123–125	455.40	455.41	455.42	-0.484	3.18
54X-1, 19–21	456.40	456.50	456.60	-1.060	3.248
54X-1, 94–96	457.15	457.25	457.35	-0.895	3.335
54X-2, 94–96	458.65	458.75	458.85	-0.437	2.588



Table T2 (continued).

Core, section, interval(cm)	Top depth CSF-A (m)	Middle depth CSF-A (m)	Bottom depth CSF-A (m)	$\delta^{13}\text{C}$ (‰ VPDB)	$\delta^{18}\text{O}$ (‰ VPDB)
54X-3, 94–96	460.15	460.25	460.35	-1.053	3.379
54X-4, 19–21	460.90	461.00	461.10	-0.137	1.962
54X-5, 19–21	462.40	462.50	462.60	-0.264	2.460
55X-1, 19–21	466.00	466.10	466.20	-0.326	2.551
55X-2, 17–19	467.48	467.58	467.68	0.340	2.305
55X-3, 19–21	469.00	469.10	469.20	-0.912	3.217
56X-1, 19–21	475.60	475.70	475.80	-0.155	2.825
56X-1, 94–96	476.35	476.45	476.55	-0.364	3.195
56X-2, 94–96	477.85	477.95	478.05	-0.264	3.240
56X-3, 94–96	479.35	479.45	479.55	0.520	1.455
56X-4, 94–96	480.85	480.95	481.05	0.568	1.621
56X-5, 19–21	481.60	481.70	481.80	0.298	1.319
56X-5, 94–96	482.35	482.45	482.55	-0.017	2.057
56X-6, 94–96	483.85	483.95	484.05	-0.194	3.256
57X-1, 19–21	485.20	485.30	485.40	-0.482	3.198
57X-2, 94–96	487.45	487.55	487.65	-0.805	3.140
57X-4, 19–21	489.70	489.80	489.90	0.353	1.338
58X-2, 94–96	495.77	495.87	495.97	-0.779	3.117
58X-3, 19–21	496.52	496.62	496.72	-1.122	3.269
58X-3, 94–96	497.27	497.37	497.47	-1.157	3.337
58X-5, 95–97	500.28	500.38	500.48	-1.539	3.194
58X-6, 19–21	501.02	501.12	501.22	-1.203	3.143
58X-6, 94–96	501.77	501.87	501.97	-0.931	3.306
58X-7, 19–21	502.52	502.62	502.72	-1.217	3.274
60X-1, 18–20	513.99	514.09	514.19	0.205	2.312
60X-CC, 19–20	514.71	514.81	514.91	-1.952	3.381
61X-1, 19–21	523.60	523.70	523.80	-1.067	3.674
61X-2, 19–21	524.60	524.70	524.80	0.127	2.129
62X-1, 19–21	533.20	533.30	533.40	-1.248	3.418
62X-1, 84–86	533.85	533.95	534.05	-1.937	3.466
62X-2, 19–21	534.70	534.80	534.90	-1.757	3.464
62X-2, 94–96	535.45	535.55	535.65	-1.392	3.533
62X-3, 19–21	536.20	536.30	536.40	-1.294	3.466
62X-3, 94–96	536.95	537.05	537.15	-1.648	3.403
62X-4, 19–21	537.70	537.80	537.90	-1.130	3.377
62X-4, 94–96	538.45	538.55	538.65	-0.898	3.332
62X-5, 19–21	539.20	539.30	539.40	-0.821	3.293
62X-5, 94–96	539.95	540.05	540.15	-1.064	3.464
62X-6, 94–96	541.45	541.55	541.65	-1.308	3.577
62X-7, 19–21	541.70	541.80	541.90	-1.744	3.414

Depths plotted in Figures F2–F6 are the depths to middle of each sample interval. VPDB = Vienna Peepee belemnite.



Table T3. Oxygen isotopic ratios ($\delta^{18}\text{O}$) and stable carbon isotopic ratios ($\delta^{13}\text{C}$) of *Nanionella flemingi* and *Uvigerina perigrina* (88 sample subset), Hole U1352B. (Continued on next page.)

Core, section, interval (cm)	Top depth CSF-A (m)	Middle depth CSF-A (m)	Bottom depth CSF-A (m)	$\delta^{18}\text{O}$ (<i>N. flemingi</i>) (‰ VPDB)	$\delta^{13}\text{C}$ (<i>N. flemingi</i>) (‰ VPDB)	$\delta^{18}\text{O}$ (<i>U. peregrina</i>) (‰ VPDB)	$\delta^{13}\text{C}$ (<i>U. peregrina</i>) (‰ VPDB)
317-U1352B-							
18H-1, 19–21	156.39	156.40	156.41	1.838	-0.460	2.162	0.380
18H-3, 19–21	159.39	159.40	159.41	3.738	-0.002	3.562	0.564
20H-3, 19–21	177.57	177.58	177.59	3.573	-0.237	3.117	0.195
21H-5, 94–96	186.64	186.65	186.66	3.252	-0.097	3.004	0.583
21H-6, 94–96	188.14	188.15	188.16	3.542	0.001	2.969	0.082
22H-2, 19–21	190.89	190.90	190.91	3.189	0.101	3.027	0.357
22H-6, 19–21	196.89	196.90	196.91	3.270	-0.085	3.066	0.311
22H-7, 19–21	198.39	198.40	198.41	3.076	0.292	2.591	0.287
23H-1, 94–96	199.64	199.65	199.66	3.145	0.243	2.818	0.304
23H-2, 19–21	200.39	200.40	200.41	3.235	0.099	2.870	0.510
23H-2, 94–96	201.14	201.15	201.16	3.916	-0.468	3.406	-0.181
23H-6, 19–21	206.39	206.40	206.41	3.489	-0.061	2.657	0.070
23H-6, 94–96	207.14	207.15	207.16	3.295	-0.107	2.755	0.406
23H-7, 19–21	207.89	207.90	207.91	3.281	0.289	3.060	0.444
24H-4, 19–21	212.89	212.90	212.91	3.506	-0.106	3.198	0.360
27H-1, 19–21	236.89	236.90	236.91	2.955	0.102	3.177	0.547
27H-5, 94–96	243.64	243.65	243.66	3.118	0.004	2.610	0.276
27H-6, 64–66	244.84	244.85	244.86	2.696	-0.148	2.662	0.335
27H-7, 19–21	245.39	245.40	245.41	2.619	-0.013	2.698	0.262
28H-1, 19–21	246.39	246.40	246.41	3.274	-0.201	2.400	0.135
28H-2, 94–96	248.57	248.58	248.59	3.603	0.065	3.270	0.002
28H-3, 19–21	249.32	249.33	249.34	3.070	-0.306	2.682	-0.336
28H-3, 34–36	249.47	249.48	249.49	2.627	-0.167	2.758	0.027
28H-3, 94–96	250.07	250.08	250.09	3.011	-0.390	2.900	-0.191
29H-2, 19–21	252.89	252.90	252.91	3.544	-1.025	3.177	-0.159
32H-5, 19–21	278.34	278.35	278.36	3.061	-0.089	2.734	-0.064
33H-1, 19–21	281.89	281.90	281.91	2.897	0.083	2.566	0.038
33H-1, 93–95	282.63	282.64	282.65	3.254	-0.233	3.231	0.028
33H-2, 19–21	283.3	283.31	283.32	3.481	-0.172	2.792	-0.099
33H-3, 19–21	284.07	284.08	284.09	3.297	-0.248	2.692	0.154
33H-4, 94–96	285.58	285.59	285.60	3.287	-0.416	3.308	0.053
33H-5, 19–21	286.33	286.34	286.35	3.371	-0.407	3.068	-0.228
34H-4, 23–25	291.00	291.01	291.02	3.188	-0.450	2.057	0.260
35H-1, 36–38	293.26	293.27	293.28	3.034	-0.130	3.087	0.327
35H-2, 19–21	294.53	294.54	294.55	2.710	0.140	2.297	0.225
36H-2, 19–21	296.69	296.70	296.71	3.137	0.296	2.652	0.282
37X-1, 94–96	297.94	297.95	297.96	2.035	0.767	2.152	0.781
37X-2, 19–21	298.69	298.70	298.71	3.043	0.035	2.989	-0.131
38X-2, 94–96	305.04	305.05	305.06	3.223	-0.212	2.675	0.346
39X-7, 19–21	321.19	321.20	321.21	3.235	0.323	3.178	0.584
40X-6, 94–96	330.34	330.35	330.36	2.607	0.161	2.223	0.460
41X-1, 19–21	331.69	331.70	331.71	3.258	-0.207	2.255	0.385
41X-2, 94–96	333.94	333.95	333.96	3.595	-0.600	2.770	0.399
41X-3, 94–96	335.44	335.45	335.46	3.389	-0.141	3.356	0.115
41X-4, 94–96	336.94	336.95	336.96	3.530	-0.278	2.860	-0.087
42X-4, 94–96	346.54	346.55	346.56	2.808	-0.203	2.741	0.199
42X-5, 18–20	347.28	347.29	347.30	1.345	0.837	1.548	0.828
42X-5, 94–96	348.04	348.05	348.06	3.008	0.092	2.708	-0.337
43X-1, 20–22	350.90	350.91	350.92	3.950	-0.962	3.896	-0.441
43X-1, 95–97	351.65	351.66	351.67	4.028	-0.836	3.998	-0.361
43X-2, 19–21	352.39	352.40	352.41	3.828	-1.254	3.419	-1.222
43X-4, 19–21	355.39	355.40	355.41	2.753	0.021	2.579	0.557
43X-6, 94–96	359.14	359.15	359.16	3.282	0.092	2.968	0.276
44X-6, 94–96	368.84	368.85	368.86	2.793	0.340	3.009	0.739
45X-3, 94–96	373.94	373.95	373.96	3.134	0.002	2.884	0.209
45X-4, 94–96	375.44	375.45	375.46	2.899	-0.100	2.850	0.253
45X-5, 19–21	376.19	376.20	376.21	3.628	0.045	3.190	0.754
46X-3, 19–21	382.77	382.78	382.79	3.046	-0.243	2.978	0.233
47X-1, 18–20	389.38	389.39	389.40	3.183	-0.132	2.362	0.178
47X-2, 19–21	390.89	390.90	390.91	2.967	-0.108	2.309	0.226
47X-2, 93–95	391.63	391.64	391.65	2.217	0.349	1.786	0.337
47X-3, 19–21	392.39	392.40	392.41	3.018	-0.269	2.198	-0.072
47X-6, 18–20	396.88	396.89	396.90	2.883	-0.591	2.981	0.091
48X-3, 94–96	402.64	402.65	402.66	2.993	-0.351	2.697	0.511
48X-4, 19–21	403.39	403.40	403.41	2.806	-0.161	2.497	0.234

Table T3 (continued).

Core, section, interval (cm)	Top depth CSF-A (m)	Middle depth CSF-A (m)	Bottom depth CSF-A (m)	$\delta^{18}\text{O}$ (<i>N. flemingi</i>) (‰ VPDB)	$\delta^{13}\text{C}$ (<i>N. flemingi</i>) (‰ VPDB)	$\delta^{18}\text{O}$ (<i>U. peregrina</i>) (‰ VPDB)	$\delta^{13}\text{C}$ (<i>U. peregrine</i>) (‰ VPDB)
49X-3, 93–95	412.23	412.24	412.25	2.224	-0.214	2.586	0.326
50X-4, 19–21	422.59	422.60	422.61	1.682	0.520	2.182	0.216
50X-7, 19–21	426.89	426.90	426.91	2.925	0.527	2.475	0.435
51X-3, 95–97	431.45	431.46	431.47	3.924	-0.400	3.367	-0.385
52X-3, 19–21	440.29	440.30	440.31	3.397	-0.296	2.872	0.200
52X-5, 93–95	444.03	444.04	444.05	1.882	0.167	1.869	0.311
52X-6, 94–96	445.54	445.55	445.56	2.647	-0.213	2.622	0.200
53X-1, 19–21	446.89	446.90	446.91	2.749	-0.001	2.322	0.024
53X-1, 95–97	447.65	447.66	447.67	2.004	0.442	1.643	0.527
53X-2, 94–96	449.14	449.15	449.16	1.953	0.071	1.649	0.280
53X-3, 94–96	450.64	450.65	450.66	1.388	0.760	1.492	0.288
53X-4, 19–21	451.39	451.40	451.41	2.605	-0.115	1.820	0.168
53X-5, 19–21	452.89	452.90	452.91	2.641	-0.160	1.910	-0.009
53X-5, 94–96	453.64	453.65	453.66	3.383	-0.262	2.588	-0.357
53X-6, 95–97	455.12	455.13	455.14	3.474	-0.848	3.291	-0.763
54X-2, 94–96	458.74	458.75	458.76	2.588	-0.437	2.683	-0.150
54X-3, 94–96	460.24	460.25	460.26	3.379	-1.053	3.354	-0.892
54X-5, 19–21	462.49	462.50	462.51	2.460	-0.264	2.360	-0.057
56X-3, 94–96	479.44	479.45	479.46	1.455	0.520	1.272	0.365
56X-5, 19–21	481.69	481.70	481.71	1.319	0.298	1.718	0.407
58X-3, 19–21	496.61	496.62	496.63	3.269	-1.122	3.362	-0.152
58X-6, 19–21	501.11	501.12	501.13	3.143	-1.203	2.596	-0.749

VPDB = Vienna Peepee belemnite.

Table T4. Bioevents reexamined in this study (*HO Pseudoemiliania lacunosa*) and reported during Expedition 317 (all others; see the “Methods” chapter [Expedition 317 Scientists, 2011a]).

Age (Ma)	Bioevent	Age reference	Depth CSF-A (m)		Core, section	
			Top	Bottom	Top	Bottom
0.29	LO <i>Emiliania huxleyi</i> (NN21 base)	Lourens et al. (2004)	112.82	121.10	12H-CC	13H-CC
0.44	HO <i>Pseudoemiliania lacunosa</i> (NN20 base)	Lourens et al. (2004)	129.77	130.34	14H-6	14H-CC
0.91	HCO <i>Reticulofenestra asanoi</i>	Lourens et al. (2004)	257.09	266.92	29H-CC	30H-CC
1.24	HO <i>Gephyrocapsa</i> >6.5 µm	de Kaenel et al. (1999)	348.59	360.08	42X-CC	43X-CC
1.26	HO <i>Gephyrocapsa</i> >5.5 µm	Lourens et al. (2004)	360.08	369.96	43X-CC	44X-CC
1.56	LO <i>Gephyrocapsa</i> >5.5 µm	Lourens et al. (2004)	412.30	427.34	49X-CC	50X-CC
1.69	HO <i>Gephyrocapsa</i> >4 µm	Lourens et al. (2004)	463.67	469.84	54X-CC	55X-CC
1.73	LO <i>Gephyrocapsa caribbeana</i>	de Kaenel et al. (1999)	469.84	484.83	55X-CC	56X-CC
	Hiatus		491.74	525.34	57X-CC	61X-CC
2.78	HO <i>Reticulofenestra ampla</i>	Kameo and Bralower (2000)	525.34	542.58	61X-CC	62X-CC
					317-U1352B-	317-U1352B-

LO = lowest occurrence, HO = highest occurrence, HCO = highest common occurrence.

